Dalton Transactions

Accepted Manuscript

ROYAL SOCIETY OF CHEMISTRY

www.rsc.org/dalton

Cd(II) based metal organic framework: a photosensitive current conductor†

Shibashis Halder,[a] Animesh Layek,[b,c] Koushik Ghosh,[a] Corrado Rizzoli,[d] Partha Pratim Ray*,[b] and Partha Roy*,[a]

[a]Department of Chemistry, Jadavpur University, Jadavpur, Kolkata-700 032, India.

E-mail: proy@chemistry.jdvu.ac.in; Tel: +91-3324572267; Fax: +91-3324146414.

[b]Department of Physics, Jadavpur University, Jadavpur, Kolkata-700 032, India.

E-mail: partha@phys.jdvu.ac.in; Tel: +91-9475237259; Fax: +91-3324138917.

[c]Department of Physics, Bejoy Narayan Mahavidyalaya, Itachuna, Hooghly-712147, India.

[d]Universita' degli Studi di Parma, Dipartimento di Chimica, Parco Area delle Scienze 17/A, I-43124 Parma, Italy.

†Electronic supplementary information (ESI) available. CCDC 1061483 for **1**. For ESI and crystallographic data in CIF or otherelectronic format see DOI .....

Abstract

A novel cadmium(II) based metal organic framework, $[Cd(3\text{-bpd})(SCN)_2]_n$ (**1**) where 3-bpd = 1,4-bis(3-pyridyl)-2,3-diaza-1,3-butadiene has been synthesized and characterized by elemental analysis, various spectroscopic techniques, TGA and single crystal X-ray diffraction analysis. X-ray analysis shows the formation of an undulated polymeric two-dimensional network parallel to the (0 -1 1) plane. Current conduction properties of **1** have been explored in dark and in the presence of light. The study shows that current conduction of the complex increases with the increase of incident light intensity. On progression of intensity of glancing radiation the photosensitivity of **1** has been increased. The time dependent light response on charge carrier conduction reveals a new epoch to **1** in the ground of optoelectronic switching application.

Introduction:

Metal-organic frameworks (MOFs) are inorganic-organic hybrid crystalline materials built from metallic nodes and organic bridging linkers to form 1-, 2- and/or 3-dimensional infinite networks.[1] Research on MOFs has become one of the fastest developing investigation areas to the researchers of chemical and materials sciences due to not only their beautiful structures and diversity in the topology[2] but also to their innumerous applications in the field of gas absorption and removal,[3] catalysis,[4] proton conduction,[5] sensing,[6] clean energy technology,[7] electronics and optoelectronics,[8] magnetism,[9] drug delivery[10] etc. MOFs with desired topology and valuable applications may be produced by judicial choice of metallic node, suitable bridging ligands and appropriate reaction conditions. MOFs are generally constructed by reaction between metal salts and N-donor ligands in the presence of bridging ligands. Commonly used N-donor ligands are neutral N-heterocyclic aromatic compounds. Bridging ligands may vary from pseudohalides to carboxylates. Thiocyanato is one of the most widely used bridging ligands. However, an N-donor neutral ligand, 1,4-bis(3-pyridyl)-2,3-diaza-1,3-butadiene(3-bpd), was reported in 2000.[11] After that a number of polymeric compounds involving 3-bpd and different transition metals, e.g. Co,[12] Cu,[13] Zn,[14] Ag,[15] Cd,[16] Hg,[17] Bi[18] etc. under different reaction conditions. The area of application of these MOFs with 3-bpd includes photoluminescence, magnetism, etc.

There are possibilities of using MOFs in the fabrication of photonic and electronic devices, but these topics have gained quite less attention than the typical several applications of nanoporous materials.[19] Over the last few years, organic polymers have been used as semiconductors, but usually they lack in thermal stability. In this scenario, MOF can be a potential candidate for use in conductivity. The electronic properties of MOFs can be tailored most importantly by using appropriate organic linkers as the organic moieties play a crucial role in shaping the overall electronic properties of the materials.[20] There are several advantages using MOFs in such devices. Firstly, MOFs have an ordered structure determined by the nature of the metal, the linkers and the reaction conditions. The strong chemical bonds formed by the self assembly process facilitate rational design[21] and also provides high thermal and chemical stability to the MOFs. Thus, pore dimensions of MOF are highly defined compared to the amorphous

porous materials and polymers. This also removes the disorder in MOFs. Disorders/defects are present in organic conductors which contribute largely to poor mobility and low carrier densities. Secondly, MOFs can be synthesized in a number of methods which are very much flexible for tuning the structure. This synthetic flexibility has been meticulously used to tune their intrinsic electrical, optical and mechanical properties. Most of the MOFs are in general insulators.[22] A few numbers of MOFs have been reported as semiconductors and very recently as Schottky Barrier Diode[23] but theoretical calculations indicate that many more are possible.[24] Host guest chemistry of MOFs has been exploited to introduce a non-native functionality by infusing guest molecules into the pores of MOF; for example, by introduction of redox molecule into the pores of MOF HKUST-1, electrical conductivity has been achieved.[25] Partial oxidation by I_2 vapor increases conductivity in MOF significantly.[26] A recent report of Zn-based MOF with tetrathiafulvalenetetrabenzoate demonstrated that the MOF exists porous in solution and exhibits very high charge mobility similar to that of some best known organic semiconductors.[27]

In this context, we report here the synthesis and characterization of a Cd(II) based 2D-metal organic framework, $[Cd(3\text{-bpd})(SCN)_2]_n$ (complex **1**) where 3-bpd = 1,4-bis(3-pyridyl)-2,3-diaza-1,3-butadiene. This complex exhibits a surprising effect of incident light on carrier conduction at an applied bias potential across it. The time dependent light response upon the current conduction exposes a novel activity of this complex in the field of optoelectronic switching application. Complex **1** has been obtained by the reaction of $Cd(NO_3)_2 \cdot 4H_2O$, KSCN and 3-bpd in methanol-water media under ambient conditions. It has been characterized by elemental analysis, different spectroscopic techniques and single crystal X-ray diffraction analysis. It has been found that depending upon the intensity of the incident light the electrical conductivity of this MOF increases accordingly.

Experimental Section

Materials and physical methods

Pyridine-3-carboxaldehyde and hydrazine hydrate were purchased from Aldrich Chemical Co. and were used as received. All other chemicals were purchased from

commercial sources and used without further purification.1,4-bis(3-pyridyl)-2,3-diaza-1,3-butadiene(3-bpd) was synthesized following the procedure reported earlier.[11] All the other chemicals including solvents were of reagent grade and were used as received without further purification. Elemental analyses (carbon, hydrogen and nitrogen) were performed using a Perkin−Elmer 240C elemental analyzer. FT-IR spectra were obtained on a Perkin Elmer spectrometer (Spectrum Two) with the samples by attenuated total reflectance (ATR) technique. Powder X-ray diffraction (PXRD) patterns of the samples were recorded on a Bruker D8 Discover instrument using Cu−Kα (λ = 1.5406 Å) radiation. FESEM image was taken on FEI made instrument (model number INSPECT F50). Thermal analysis (TGA) was carried out using a METTLER TOLEDO TGA 850 thermal analyzer under nitrogen atmosphere (flow rate: 50 cm^3 min^{-1}) at the temperature range 25°C-800°C with a heating rate of 2 °C /min.

Synthesis of $[Cd(3\text{-bpd})(SCN)_2]_n$

An aqueous solution (4.0 mL) of potassium thiocyanate (2.0 mmol, 0.194 g) was added to a methanolic solution (4.0 mL) of 1,2-bis-(pyridine-3-ylmethelyne)hydrazine (3-bpd) (1.0 mmol, 0.210 g) taken in a beaker and stirred for 30 minute to mix well. $Cd(NO_3)_2{\cdot}4H_2O$ (1.0 mmol, 0.308 g) was dissolved in 4.0 mL of water in a test tube. Then previously prepared mixed ligand solution was slowly and carefully layered with the aqueous $Cd(NO_3)_2$ solution using 5.0 mL of 1:1 *v*/*v* of water and methanol mixture as buffer. The yellow needle-shaped crystals suitable for single crystal X-ray analysis were obtained after few days. The crystals were collected and washed with a methanol-water mixture and dried in vacuum. (Yield= 76%). Anal. Calc.(%) for $C_{14}H_{10}CdN_6S_2$: C, 38.28; H, 2.28; N, 19.14. Found: C, 38.12; H, 2.39; N, 2.21.

Crystallographic Data Collection and Refinement

A suitable yellow colored single crystal of the compound was mounted on the tips of glass fibers coated with commercially available super glue. X-ray single crystal data were collected at room temperature using a Bruker APEX II diffractometer, equipped with a fine-focus, sealed tube X-ray source with graphite monochromated Mo−Kα radiation (λ = 0.71073 Å). The data were integrated using a SAINT program[28] and the

absorption correction was made with SADABS. The structure was solved by SIR97[29a] using direct methods and refined by full matrix least-squareson F^2 using SHELXL-97[29b] with anisotropic displacement parameters for all non-hydrogen atoms. All the hydrogen atoms were fixed geometrically and placed in ideal positions. The coordinates, anisotropic displacement parameters, and torsion angles for all three compounds are submitted as Supplementary Information in CIF format. Data collection and structure refinement parameters are given in Table 1.

Electrical characterization

In this study, complex **1** was deposited as a thin film by preparing a well dispersed solution of **1** in DMF. First, complex **1** was mixed with DMF in right proportion and was sonicated for 30 minute. To develop the thin film, an ITO coated glass substrate was cleaned by acetone, ethanol and deionized water with the help of an ultra-sonicator and dried. On the top of the cleaned ITO coated substrate, a well dispersed solution was spun firstly at 800 rpm for 2 min and thereafter, at 1400 rpm for 10 min, with the help of SCU 2700 spin coating unit. Before depositing the aluminum electrode as front contact, the as-deposited thin film was dried in a vacuum oven at 120°C. For the characterization of the developed thin film, thickness was measured by surface profiler as 800 nm. The aluminum electrodes were deposited on to the film through shadow mask by a Vacuum Coating Unit 12A4D of HINDHIVAC under pressure 10^{-6} Torr. The effective area of the film was maintained as 7.065×10^{-2} cm^{-2}. For electrical characterization, the current-voltage characteristic was measured in dark and under illumination from AM1.5 radiation, with the help of a Keithley 2400 source meter by two-probe technique. A schematic diagram of the system is given in the Supplementary Information (Fig. S1). The current-voltage (I-V) characteristics of the material were measured in dark and under illumination from AM 1.5 radiation. All the preparation and measurements were performed at room temperature and under ambient conditions. To measure the light response on conductivity the system was set up under exposed of light and the I-Vs were recorded by varying intensity (60 $mWcm^{-2}$, 70 $mWcm^{-2}$ and 80 $mWcm^{-2}$).

Results and discussion

Description of crystal structure of complex 1

Single crystals of complex **1** were obtained by slow evaporation of a methanol/water solution. The compound crystallizes in the triclinic P-1 space group from. An ORTEP drawing of the asymmetric unit of the complex is shown in Fig. 1. Selected bond lengths and bond angles are given in Table 2. The asymmetric unit consists of one cadmium(II) ion, one half of a 3-bpd ligand, and one thiocyanato ion. The cadmium atom lies on centre of symmetry and displays an elongated octahedral coordination geometry provided by four nitrogen atoms of two 3-bpd ligands and two thiocyanato ions forming the equatorial plane, and two sulfur atoms of different thiocyanato ions at the apices. The 3-bpd ligand is nearly planar (r.m.s. deviation = 0.0431 Å) and acts as a bridge between adjacent metal centers through the pyridine N atoms. The thiocyanato ions adopt a μ-$_{1,3}$ bridging mode resulting in the formation of eight-membered metallacycles connected into polymeric chains parallel to the *a* axis (Fig. 2), which are further linked by the bridging role of the 3-bpd ligands into two-dimensional undulated network parallel to the (0 -1 1) plane (Fig. 3). In the crystal, packing is enforced by interlayer π...π stacking interactions (Fig. 4) involving the pyridine rings, with centroid-to-centroid distance, perpendicular interplanar distance, and offset of 3.722(3), 3.4733(17), and 1.339(7) Å, respectively.

Fluorescence Spectra

MOFs have been used as photoluminescent materials. MOFs of Zn^{2+} and Cd^{2+} display interesting luminescence property. The fluorescence spectra of the ligand and complex **1** were recorded at the solid state. The emission peak of 3-bpd was observed at 363 nm when it was excited at 240 nm as reported earlier.[12a] This may be due to the π*–n or π*–π transition. Complex **1** showed an emission band at 390 nm on excitation at 240 nm (Fig. S2). It is known that emission of d^{10} metal ions could not be observed due to metal centered MLCT or LMCT transition. Thus, the emission of complex **1** may be attributed to the intra-ligand transitions.

Thermogravimetric analysis

To check the thermal stability of complex **1**, thermogravimetric analysis was performed with the powdered sample within the temperature range 25°C to 800°C under nitrogen flow [Fig. S4]. There was no appreciable loss of mass up to 200°C which confirmed the framework stability of the material. As thin coating on ITO glass surface involved a drying temperature of 120°C. TGA study suggests that the complex retained its stability during thin film preparation.

FT-IR spectroscopy

FT-IR spectra of complex **1** before and after heating at 120 °C were recorded using ATR method in order to ensure the stability of the complex (Fig. S5). Complex **1** before heating at 120 °C shows bands at 2103 cm^{-1} for ν(SCN) and the band at 1623 cm^{-1} may be attributed to the presence of C=N moiety. IR spectrum of complex **1** after heating at 120 °C exhibits very similar spectrum as comparison to the IR spectrum of complex **1** before heating at 120 °C. This indicates that the complex is stable at 120 °C.

Powder X-ray Diffraction

In order to confirm the thermal stability of the complex, powder X-ray diffraction (PXRD) analyses were performed on bulk complex **1** and the complex after heating to 120 °C (Fig. 5). The excellent agreement between the PXRD peak pattern of bulk of complex **1** and simulated PXRD pattern from single crystal X-ray diffraction data of **1** indicates that the bulk material actually has same structure as that obtained from single crystal diffraction study. Fig. 5 shows that the PXRD pattern of the bulk material (b) and the material heated up to 120 °C (c) exhibit identical peak positions and intensities indicating that complex maintains its structure after its deposition to ITO glass.

Electrical characterization and photosensitivity

Since complex **1** has high luminosity with excitation (~ 240 nm) and emission wavelength (~ 390 nm), there must have some impact of incident radiation on the charge transport phenomena within the thin film of this complex. The current-voltage (I-V)

characteristics of configuration ITO/complex **1**/Al were recorded under dark and under illumination of incident light by varying power density 60 $mWcm^{-2}$, 70 $mWcm^{-2}$ and 80 $mWcm^{-2}$ respectively (Fig. 6). Determining the slope of these linear plots the conductivity of the complex **1** was calculated to be 4.53×10^{-7} S cm^{-1} (at dark); 1.93×10^{-6} S cm^{-1} (at 60 $mWcm^{-2}$); 2.25×10^{-6} S cm^{-1} (at 70 $mWcm^{-2}$) and 2.52×10^{-6} S cm^{-1} (at 80 $mWcm^{-2}$) respectively. In this regards the effective area and the thickness of the film was measured as 7.065×10^{-2} cm^2 and 800 nm respectively. Hence the photosensitivity of the material under incident radiation of power densities 60$mWcm^{-2}$, 70$mWcm^{-2}$ and 80$mWcm^{-2}$ were estimated to be 5.56, 4.96, and 4.26 sequentially (the corresponding variation plot was given in supplementary Fig. S6). With the above result in mind the time dependent light response on electric current through the material was measured many times at constant bias voltage of 1.0 V by switching the light (intensity 80$mWcm^{-2}$) on and off repeatedly and sequentially for the interval 50 second. Fig. 7 represents the corresponding array (for switch on and off condition), which indicates that the material has good sensitivity to the exposure of light.

The study on electrical measurement of MOFs under different conditions is in special attention to the scientists.[30] However, mechanism for photosensitive current conduction of the MOF (complex **1**) is not clear. Probably more data are required for its elucidation.

To trace out any effect of heat on carrier transport the photocurrent through the device was measured after each interval of 60 second under constant exposure of light of intensity 80 $mWcm^{-2}$ at constant bias 1V (Fig. S8). It was observed from this plot that the magnitude of current has been deteriorated little bit rather improvement, as long as the device is being exposed by the incident light. This deviation is negligibly small, which might be due to the unavoidable light induced degradation of the material.

To eliminate other possibilities of artifacts in the measurement, firstly, ITO/Al junction was prepared without MOF and it was characterized. I-V characteristics of this junction were measured under dark and light conditions (Fig. S9). It can be seen that there is no effect of light illumination on the current for this junction. To examine whether the ligand (3-bpd) of MOF is giving any photoresponse, ITO/3-bpd/Al junction was fabricated and its I-V characteristics were measured under light and dark conditions

(Fig. S10). This device also doesn't show any photoresponse within the measured voltage range. I-V characteristics of a previously reported Cd(II) based MOF was measured in ITO/MOF/Al structure.[23] For this sample, photocurrent and dark current are same up to 10 V. This sample doesn't show any photoresponse. In contrast with these results, complex **1** shows some positive photoresponse. Above all, this photosensing behavior is exceptional and represents an important step toward the use of complex **1** in optoelectronic switching devices and photovoltaics. This field of research with MOF based compounds is just started to explore, in which our complex has a potential promise.

Conclusion

In this paper, we have been able to synthesize and characterize a Cd-based MOF $[Cd(3\text{-bpd})(SCN)_2]_n$ with a bidentate pyridine derivative and thiocyanato ligands. Current conduction of the material has been analyzed after preparing a thin film coated on ITO glass with the complex in dark and in the presence of light. The results show that there is an increment of current conduction in the presence of light. The photoconductivity increased depending upon the increment of power density of incident light. This behavior led us to measure the time dependent photo-response through the thin film of the synthesized MOF. The photo-response curve shows two distinct operational regions (On and Off) at a constant bias voltage, which is the signature of light sensing behavior. This could introduce the Cd based MOF complex as a promising candidate in application of optoelectronic switching devices.

Acknowledgements

PR wishes to thank Department of Science and Technology, New Delhi for financial supports. SH wishes to thank CSIR, New Delhi for his fellowship.

References

1 H. C. J. Zhou and S. Kitagawa, *Chem. Soc. Rev.,* 2014, **43**, 5415.

2 (a) M. Li, D. Li, M. O'Keeffe and O. M. Yaghi, *Chem. Rev.*, 2013, **114**, 1343; (b) Q. Chen, F. Jiang, D. Yuan, G. Lyu, L. Chen and M. Hong, *Chem. Sci.*, 2014, 483.

3 (a) J. A. Mason, M. Veenstra and J. R. Long, *Chem. Sci.*, 2014, **5**, 32; (b) S. Chaemchuen, N. A. Kabir, K. Zhou and F. Verpoort, *Chem. Soc. Rev.*, 2013, 9304; (c) J. Liu, P. K. Thallapally, B. P. McGrail, D. R. Brown and J. Liu, *Chem. Soc. Rev.*, 2012, **41**, 2308; (d) K. Sumida, D. L. Rogow, J. A. Mason, T. M. McDonald, E. D. Bloch, Z. R. Herm, T. H. Bae and J. R. Long, *Chem. Rev.*, 2012, **112**, 724; (e) J. R. Li, J. Sculley and H. C. Zhou, *Chem. Rev.*, 2012, **112**, 869; (f) E. Barea, C. Montoro and J. A. R. Navarro, *Chem. Soc. Rev.*, 2014, **43**, 5419.

4 (a) M. Eddaoudi, D. F. Sava, J. F. Eubank, K. Adil and V. Guillerm, *Chem. Soc. Rev.,* 2015, **44**, 228; (b) J. Liu, L. Chen, H. Cui, J. Zhang, L. Zhang and C.-Y. Su, *Chem. Soc. Rev.,* 2014, **43**, 6011; (c) T. Zhang and W. Lin, *Chem. Soc. Rev.,* 2014, **43**, 5982; (d) A. Dhakshinamoorthy and H. Garcia, *Chem. Soc. Rev.,* 2014, **43**, 5750; (e) S. H. A. M. Leenders, R. Gramage-Doria, B. d. Bruin and J. N. H. Reek, *Chem. Soc. Rev.* DOI: 10.1039/c4cs00192c.

5 (a) M. Yoon, K. Suh, S. Natarajan and K. Kim, *Angew. Chem., Int. Ed.*, 2013, **52**, 2688; (b) P. Ramaswamy, N. E. Wong and G. K. H. Shimizu, *Chem. Soc. Rev.,* 2014, **43**, 5913; (c) S. Horike, D. Umeyama and S. Kitagawa, *Acc. Chem. Res.*, 2013, **46**, 2376.

6 L. E. Kreno, K. Leong, O. K. Farha, M. Allendorf, R. P. Van Duyne and J. T. Hupp, *Chem. Rev.*, 2012, **112**, 1105.

7 N. Linares, A. M. Silvestre-Albero, E. Serrano, J. Silvestre-Albero and J. García-Martínez, *Chem. Soc. Rev.*, 2014, **43**, 7681.

8 V. Stavila, A. A. Talin and M. D. Allendorf, *Chem. Soc. Rev.*, 2014, **43**, 5994.

9 (a) P. Mahata,C. M. Draznieks,P. Roy and S. Natarajan, *Cryst. Growth Des.*, 2013, **13**, 155; (b) P. Mahata, S. Natarajan, P. Panissod and M. Drillon, *J. Am. Chem. Soc.*, 2009, **131**, 10140.

10 (a) J. Rocca, D. Liu and W. Lin, *Acc. Chem. Res.*, 2011, **44**, 957; (b) P. Horcajada, R. Gref, T. Baati, P. K. Allan, G. Maurin, P. Couvreur, G. Féerey, R. E. Morris and C. Serre, *Chem. Rev.*, 2012, **112**, 1232; (c) K. E. deKafft, Z. G. Xie, G. H. Cao, S. Tran, L. Q. Ma, O. Z. Zhou and W. Lin, *Angew. Chem., Int. Ed.*, 2009, **48**, 9901.

11 Y. B. Dong, M. D. Smith, R. C. Layland, and H. C. zurLoye, *Chem. Mater.*, 2000**, 12**, 1156.

12 (a) D. K. Maity, B. Bhattacharya, R. Mondal and D. Ghoshal, *CrystEngComm.*, 2014, **16**, 8896; (c) Y. B. Dong, M. D. Smith and H. C.zurLoye, *J. Solid State Chem.*, 2000, **155**, 143.

13 K. Drabent and Z.Ciunik, *Cryst. Growth Des.*, 2009, **9**, 3367.

14 (a) J. Zhou,L. Du,Y. F. Qiao, Y. Hu, B. Li, L. Li, X. Y. Wang, J. Yang, M. J. Xie and Q. H. Zhao, *Cryst. Growth Des.*, 2014, **14**, 1175; (b) Z. R. Ranjbar, A. Morsali and P.Retailleau, *Inorg. Chim. Acta.*, 2011, **376**, 486; (c) F. Bigdeli, A. Morsali and P.Retailleau, *Polyhedron.*, 2010, **29**, 801; (d) M. Khanpour, A. Morsali and P.Retailleau, *Polyhedron.*, 2010, **29**, 1520; (e)M. G. Amiri, G. Mahmoudi, A. Morsali, A. D. Hunter and M. Zeller, *CrystEngComm.*, 2007, **9**, 686.

15 D. Dang, Y. Zheng, Y. Bai, X. Guo, P. Ma and J.Niu, *Cryst. Growth Des.*, 2012, **12**, 3856.

16 (a) Y. B. Dong, M. D. Smith and H. C. zurLoye, *Inorg. Chem.*, 2000, **39***,* 4927; (b) B. Bhattacharya, R. Dey, D. K. Maity and D. Ghoshal, *CrystEngComm.*, 2013, **15**, 9457.

17 (a) G. Mahmoudi, A. Morsali and M. Zeller, *Inorg.Chim.Acta.*,2009, **362**, 217; (b) G. Mahmoudi and A.Morsali, *Polyhedron*, 2008, **27**, 1070.

18 N. Soltanzadeh and A. Morsali, *Polyhedron*, 2009, 28, 703.

19 M. D. Allendorf, A. Schwartzberg, V. Stavila and A. A. Talin, *Chem. Eur. J.*, 2011, **17**, 11372.

20 G. Givaja, P. A. Ochoa, C. J. Gómez-García and F. Zamora, *Chem. Soc. Rev.*, 2012, **41**, 115.

21 M. Meilikhov, S. Furukawa, K. Hirai, R. A. Fischer and S. Kitagawa, *Angew.*

Chem. Int. Ed., 2013, **52**, 341.

22 D. M. D'Alessandro, J. R. R. Kanga and J. S. Caddy, *Aust. J. Chem.*, 2011, **64**, 718.

23 B. Bhattacharya, A. Layek, M. M. Alam, D. K. Maity, S. Chakrabarti, P. P. Ray and D. Ghoshal, *Chem. Commun.,* 2014, **50**, 7858.

24 C. G. Silva, A. Corma and H. Garcia, *J. Mater. Chem.*, 2010, **20**, 3141.

25 A. A. Talin, A. Centrone, A. C. Ford, M. E. Foster, V. Stavila, P. Haney, R. A. Kinney, V. Szalai, F. El Gabaly, H. P. Yoon, F. Leonard and M. D. Allendorf, *Science*, 2014, **343**, 66.

26 Y. Kobayashi, B. Jacobs, M. D. Allendorf and J. R. Long, *Chem. Mater.*, 2010, **22**, 4120.

27 T. C. Narayan, T. Miyakai, S. Seki and M. Dincă, *J. Am. Chem. Soc.*, 2012, **134**, 12932.

28 APEX-II, SAINT and SADABS. Bruker AXS Inc., Madison, WI, 2008.

29 (a) A. Altomare, M. C. Burla, M. Camalli, G. Cascarano, C. Giacovazzo, A. Guagliardi, A. G. G. Moliterni, G.Polidori and R. Spagna, *J. Appl. Cryst.*, 1999, **32**, 115; (b) G. M. Sheldrick, *Acta Cryst.,* 2008, **A64**, 112

30 (a) L. Sun, C. H. Hendon, M. A. Minier, A. Walsh and M. Dincă, J. Am. Chem. Soc., 2015, **137**, 6164; (b) M. C. So, G. P. Wiederrecht, J. E. Mondloch, J. T. Hupp and O. K. Farha, *Chem. Commun.,* 2015, **51**, 3501; (c) R. Rahimi, S. Shariatinia, S. Zargari, M. Y. Berijani, A. Ghaffarinejad and Z. S. Shojaie, *RSC Adv.*, 2015, **5**, 46624; (d) H.-J. Son, S. Jin, S. Patwardhan, S. J. Wezenberg, N. C. Jeong, M. So, C. E. Wilmer, A. A. Sarjeant, G. C. Schatz, R. Q. Snurr, O. K. Farha, G. P. Wiederrecht and J. T. Hupp, *J. Am. Chem. Soc*., 2013, **135**, 862; (e) C. Y. Lee, O. K. Farha, B. J. Hong, A. A. Sarjeant, S. B. T. Nguyen and J. T. Hupp, *J. Am. Chem. Soc*., 2011, **133**, 15858.

Table 1. Crystal data for complex **1**

Formula	$C_{14}H_{10}CdN_6S_2$
formula weight	438.83
crystal system	triclinic
space group	P -1
a/Å	6.0349(13)
b/Å	8.2409(19)
c/Å	8.7848(19)
α/°	110.302(4)
β/°	100.984(4)
γ/°	93.003(3)
V/Å^3	398.90(15)
Z	1
Dc/g cm^{-3}	1.827
μ/mm^{-1}	1.637
F(000)	216
θ range/°	2.54-25.25
reflections collected	2411
unique reflections	1444
reflections I > 2σ(I)	1350
R_{int}	0.0178
goodness-of-fit (F2)	1.071
R_1 (I > 2σ(I))[a]	0.0321
wR_2[a]	0.0764
Δρ max/min/e Å^3	-0.43,0.39

[a] $R_1 = \Sigma \left| |F_o| - |F_c| \right| / \Sigma |F_o|$, $wR_2 = [\Sigma(w(F_o^2 - F_c^2)^2)/\Sigma w(F_o^2)^2]^{1/2}$

Table 2: Selected bond lengths (in Å) and selected bond angles (in degree) of Complex **1**

Cd1−N3	2.318(3)
Cd1−N1	2.367(3)
Cd1−S1	2.7846(11)

N3−Cd1−N3^{i}	180(-)
N3−Cd1−N1	93.45(11)
N3^{i}−Cd1−N1	86.55(11)
N1−Cd1−N1^{i}	180(-)
N3−Cd1−S1^{iii}	91.75(9)
N3−Cd1−S1^{ii}	88.25(9)
N1−Cd1−S1^{iii}	89.38(7)
N1−Cd1−S1^{ii}	90.62(7)
S1^{ii}− Cd1−S1^{iii}	180(-)
C7^{ii}−S1^{ii}−Cd1	101.83(13)
C5−N1−Cd1	118.6(2)
C1−N1−Cd1	124.7(2)
C7−N3−Cd1	163.3(3)

Symmetry codes: (i) -x, -y, -z; (ii) -1+x, y, z; (iii) 1-x, -y, -z.

Figures

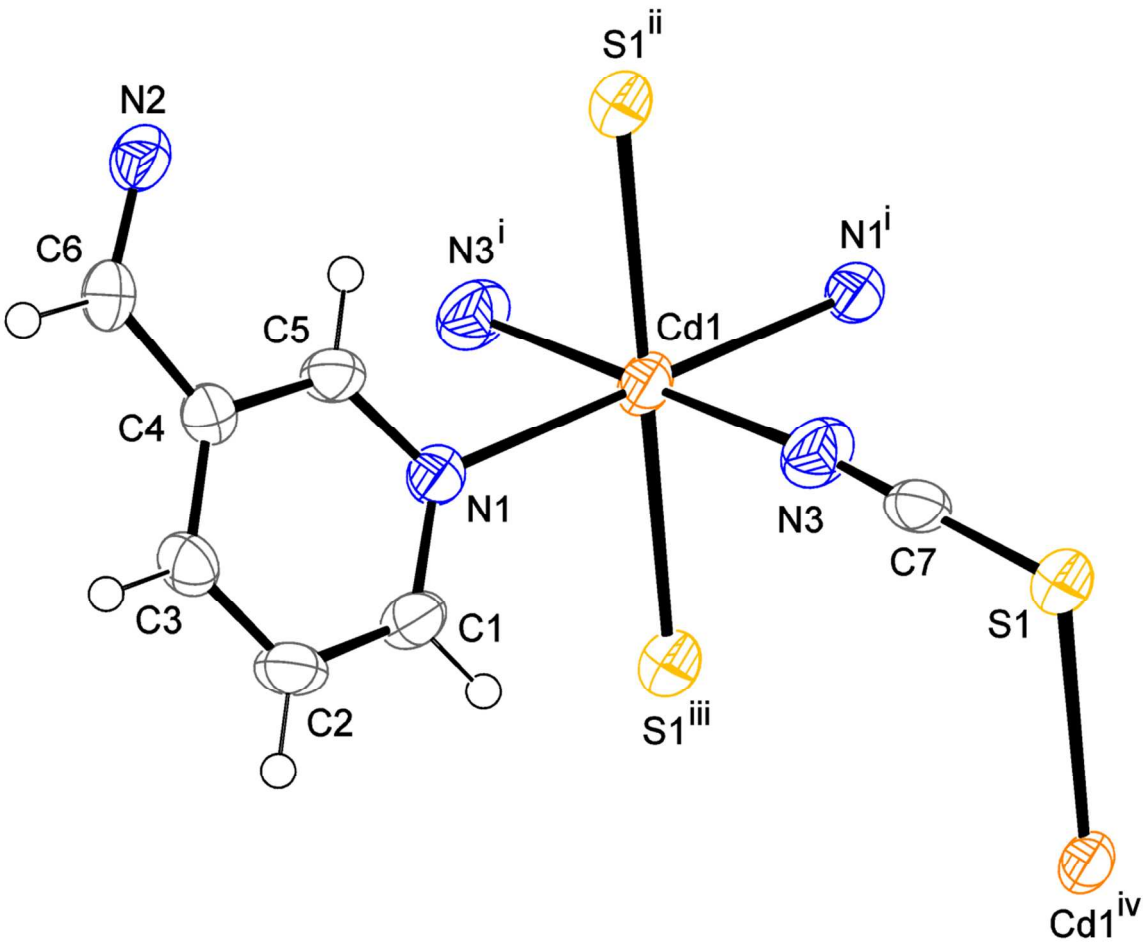

Fig. 1: ORTEP diagram of the asymmetric unit of complex **1**, with displacement ellipsoids drawnat the 50% probability level. Symmetry codes: (i) -x, -y, -z; (ii) -1+x, y, z; (iii) 1-x, -y, -z: (iv) 1+x, y, z.

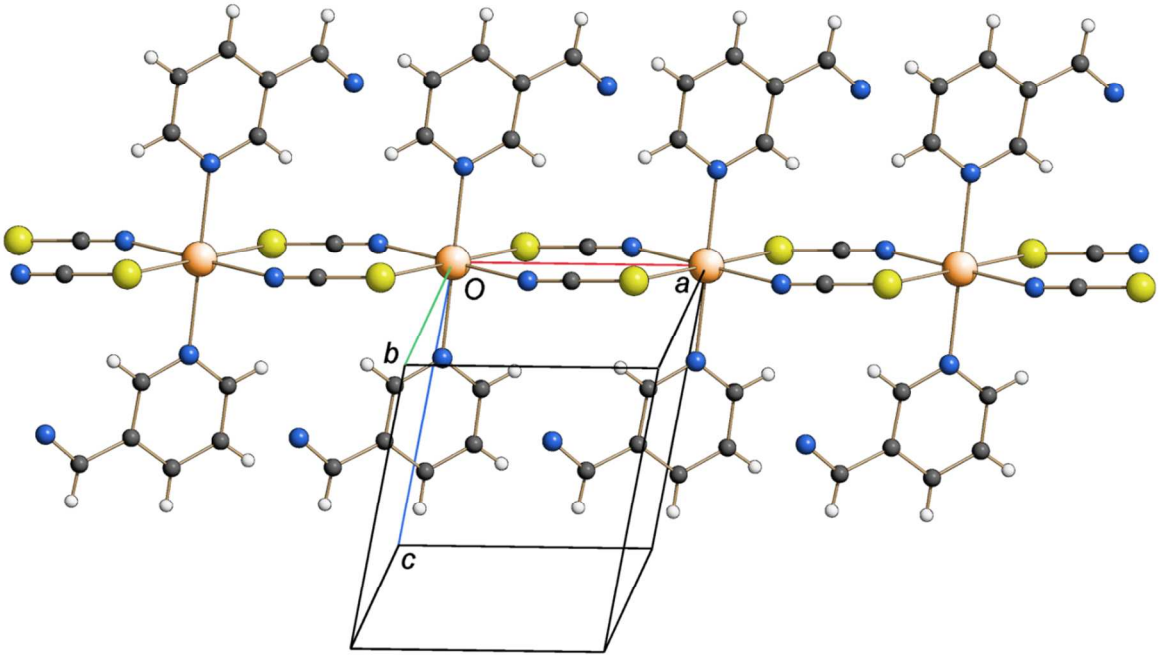

Fig. 2: The polymeric chain of complex **1** extending along the *a* axis.

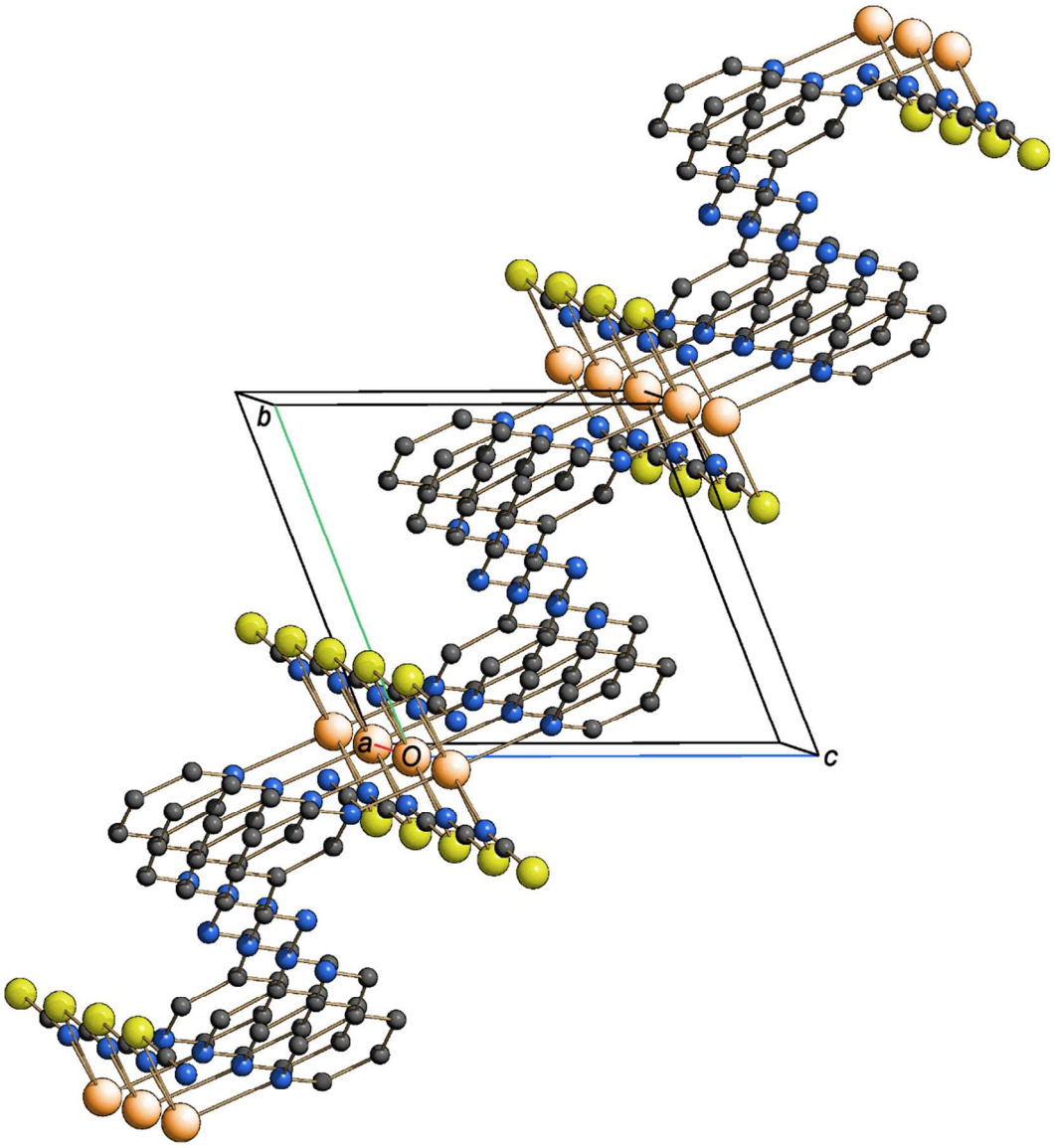

Fig. 3: Partial crystal packing of complex **1** showing an undulated polymeric layer parallel to the (0 -1 1) plane. Hydrogen atoms are omitted for clarity.

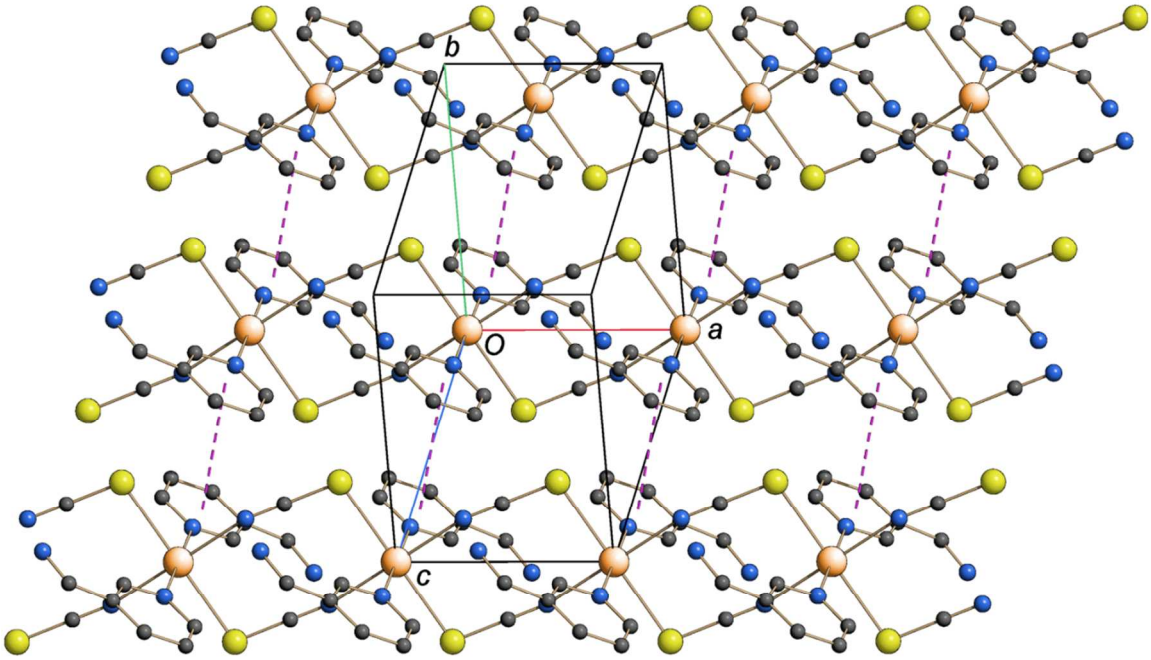

Fig. 4: Crystal packing of complex **1** showing the interlayer π...π interactions (dashed lines). Hydrogen atoms are omitted for clarity.

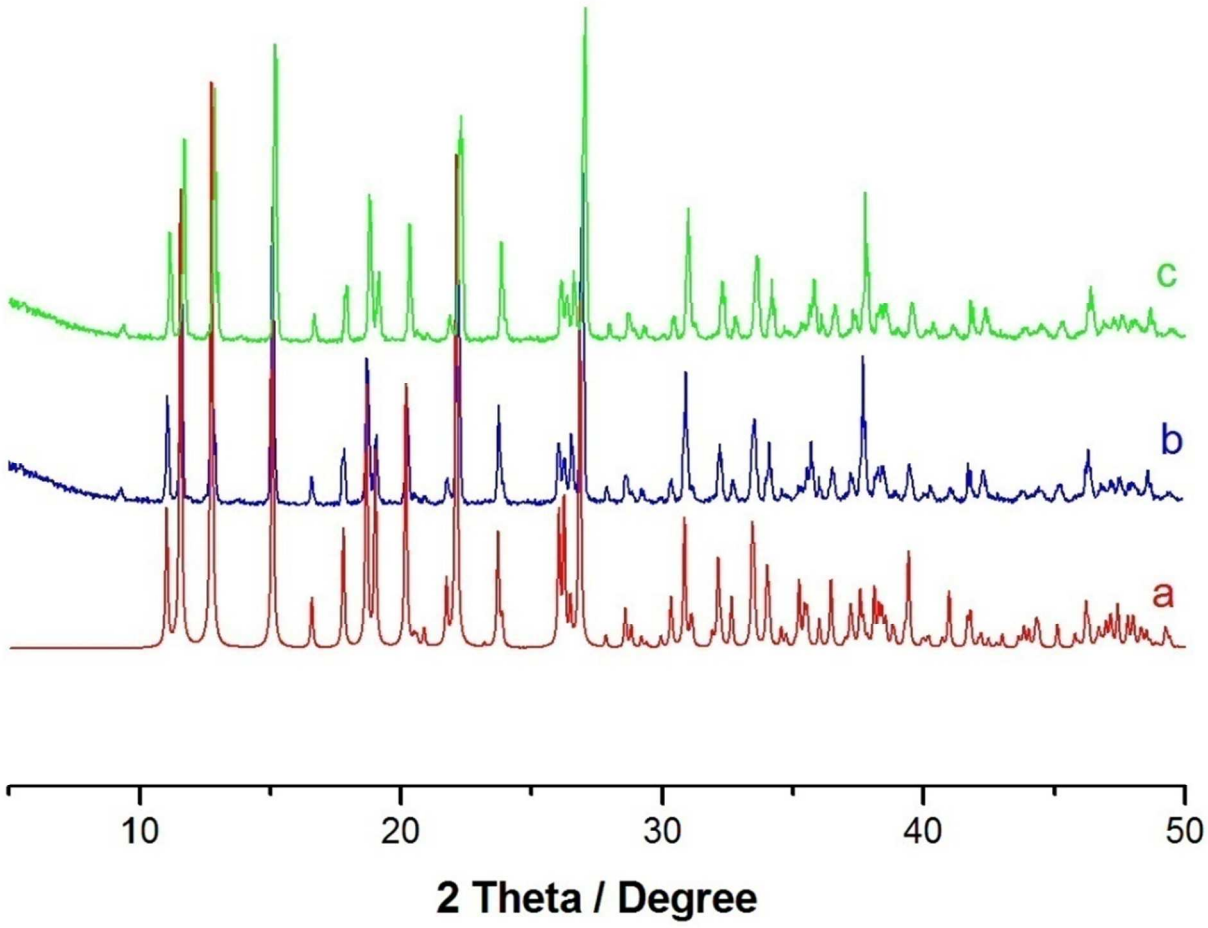

Fig. 5: PXRD patterns of complex **1** in different states. (a) Simulated from X-ray single crystal data, (b) bulk material, (c) after heating at 120 °C

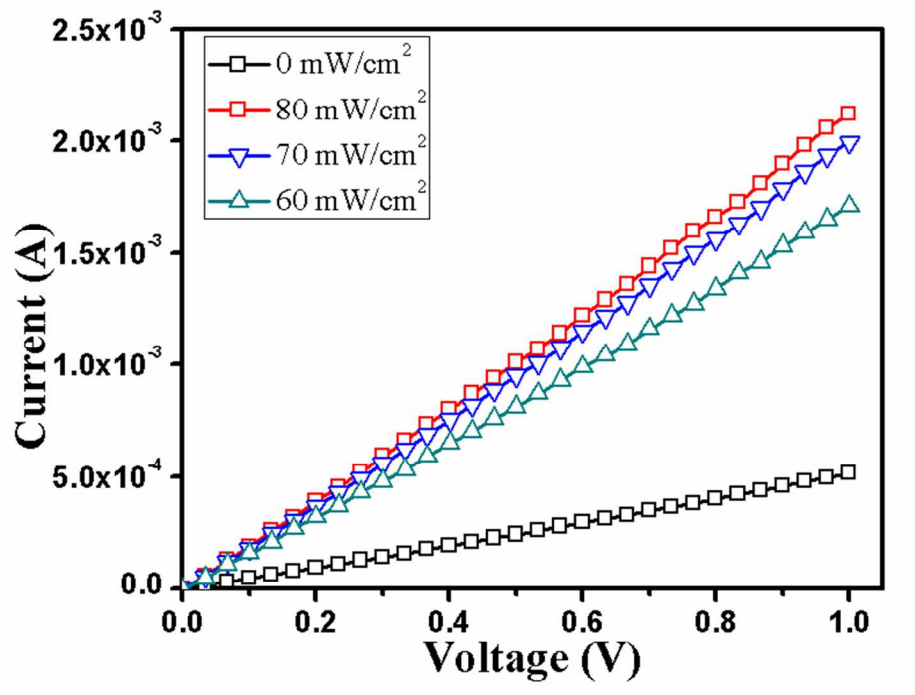

Fig. 6: Current- Voltage characteristics under dark (zero $mWcm^{-2}$) and light illumination (of intensity 80, 70 and 60 $mWcm^{-2}$) conditions

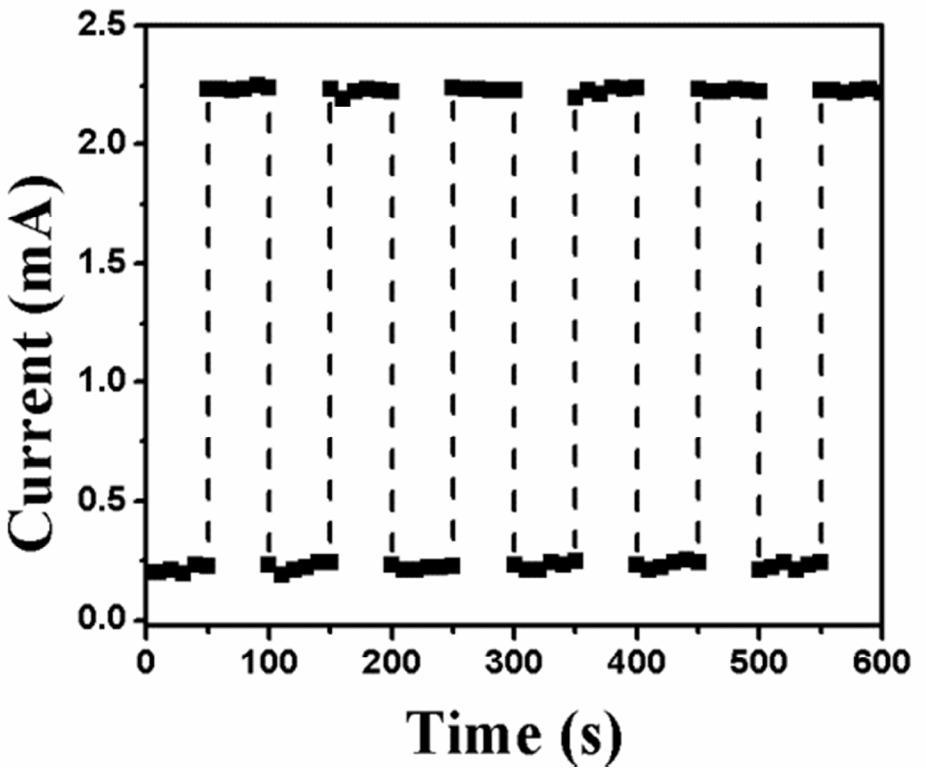

Fig. 7: Electric current, at bias voltage 1.0 V for the on and off conditions of incident light (80 mWcm^{-2}).

Graphical Abstract

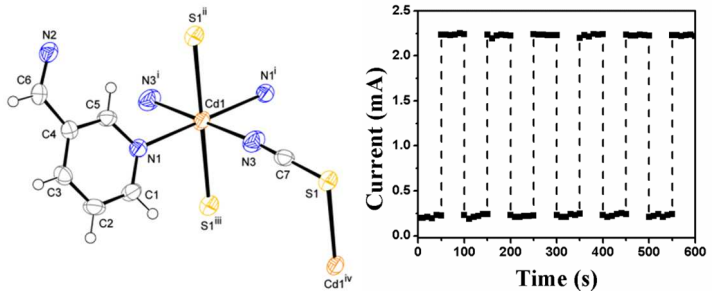

A photoresponsive MOF, $[Cd(3\text{-bpd})(SCN)_2]_n$ shows 5.56 times enhancement in current conduction in the presence of light with comparison to dark.